



## **Sensitivity of air quality indicators to emission inventories (EDGAR, EMEP, CAMS-REG) in Europe through FAIRMODE benchmarking methodology.**

5 Alexander de Meij<sup>1</sup>, Cornelis Cuvelier<sup>2♦</sup>, Philippe Thunis<sup>2</sup>, Enrico Pisoni<sup>2</sup>, Bertrand Bessagnet<sup>2</sup>

<sup>1</sup>MetClim, Varese, 21025, Italy

<sup>2</sup> European Commission, Joint Research Centre (JRC), 21027, Ispra, Italy

♦retired with Active Senior Agreement

*Correspondance to* : Philippe Thunis ([philippe.thunis@ec.europa.eu](mailto:philippe.thunis@ec.europa.eu))

10



## Abstract

15 This study evaluates the sensitivity of four different emission inventories (EDGAR 5.0, EMEPG, CAMS version 2.2.1 and CAMS version 4.2 + condensables) on calculated air quality indices using the EMEP chemistry transport model. Emissions are reduced by 25% and 50% for different air pollutants for six cities and two regions in Europe to study the impact on particulate matter (PM) ozone (O<sub>3</sub>) formation. We performed the simulations for the year 2015 over Europe.

20 Emission at each location for all precursors are quite consistent for EMEP and CAMS inventories (as i.e. all these inventories share the same country total emissions), while EDGAR (being developed using a completely independent approach) generally show different urban scale emissions. Similar emission totals can however hide large variations in sectorial allocation. Our results stress the importance of the sectorial repartition of the emissions, given their different vertical distribution. In terms of non-linear behavior, the relationship between emission reduction and PM<sub>10</sub> concentration change shows the largest non-linearity for NO<sub>x</sub> and in a lesser extend for NH<sub>3</sub> whereas it remains mostly linear for the other precursors (VOC, SO<sub>x</sub> and PPM).

25 For O<sub>3</sub>, NO<sub>x</sub> emission reductions are the most efficient, likely because of the urban focus of this work and the abundance of NO<sub>x</sub> emission in this type of areas. In terms of non-linear behaviour, the relationship between emission reduction and O<sub>3</sub> concentration change shows the largest non-linearity for NO<sub>x</sub> (concentration increase) and a quasi linear behaviour for VOC (concentration decrease). Potencies and potentials can show differences that are as large between inventories (EMEPC2 vs EMEPG) than between inventory versions (EMEPC2 vs. EMEPC42C). Precursor emission ratios (e.g. VOC/NO<sub>x</sub> for ozone or NO<sub>x</sub>/NH<sub>3</sub> for PM<sub>10</sub>) show important differences among emission inventories. This emphasizes the importance of the accuracy of emission estimates since these differences can lead to changes of chemical regimes, directly affecting the responses of O<sub>3</sub> or PM<sub>10</sub> concentrations to emission reductions.

35 It is also important to understand that the choice of the indicator (for example mean or P95 values) can lead to different outcomes. It is therefore important to assess the variability of the results around the choice of the indicator to avoid misleading interpretations of the results.

40 This work takes part of the Forum for Air Quality Modelling (FAIRMODE), that provides air quality modellers a permanent forum to address air quality modelling issues (<https://fairmode.jrc.ec.europa.eu>).

## 1. Introduction

45 Despite the application of an increasingly strict EU air quality legislation, air quality remains problematic in large parts of Europe (EEA, 2020). This becomes even more crucial now that more stringent recent WHO guideline values (WHO, 2021) as well as the recently proposed EU limit values (EC, 2022) have acknowledged that air pollution can have negative impacts on health at much lower concentration levels for air pollutants such as PM<sub>10</sub>, PM<sub>2.5</sub> and NO<sub>x</sub>. To comply with these higher-ambition limit values, a better understanding of the potential impacts of emission abatement measures on air quality is required. Air chemistry transport models (CTMs) are used to calculate air pollutant concentration levels where no observations are available, and to perform emission



reduction scenarios that help scientists and policymakers to understand which and how much of the emissions should be reduced to improve air quality. Over the years, CTMs continuously evolved by implementing newer, better chemical and dynamical atmospheric processes, and improved higher spatial grid resolution to capture fine-scale features driven by land surface characteristics (De Meij et al., 2015, 2018).

Many studies have investigated the importance of understanding the uncertainties associated to certain processes when air chemistry models are used to support policy making, such as meteorological input (De Meij et al., 2009a and references therein), aerosol chemistry (Thunis et al., 2021a, Clappier et al., 2021), model resolution (De Meij et al., 2007), or the emissions used as input to the model (Thunis et al., 2021b and references therein). Many of these topics are addressed in the frame of the Forum for Air Quality Modelling (FAIRMODE) (<https://fairmode.jrc.ec.europa.eu/home/index>) that provides air quality modellers with a permanent forum to address air quality modelling issues, such as the impact of the uncertainties of emission inventories on calculated air quality concentrations. One of FAIRMODE's goal is to assess the sensitivity of the model responses to emission reductions in general. Several factors are assessed to explain the variability in calculated air pollutant responses to emission changes, such as emissions, model resolution and meteorological input. In this study, the robustness of the model responses to emission reductions is assessed when the emission input data are changed. It is indeed crucial to better understand the uncertainties associated to the emission inventories and how these uncertainties impact the level of accuracy of the resulting air quality modelling concentration changes (Georgiou et al., 2020), a key model output for designing air quality plans.

In the light of the above, we investigate in this work the robustness of model responses to emission changes with a CTM based on different emission inventories and use specific indicators for the analysis. To this end, we perform simulations over Europe with the air chemistry transport model EMEP (Simpson et al., 2012), fed by four emission inventories, namely EDGAR 5.0, EMEPG, CAMS version 2.2.1 and CAMS version 4.2 + condensables. We reduce the anthropogenic emissions in six cities (Brussels, Madrid, Rome, Bucharest, Berlin and Stockholm) and 2 regions (Po Valley Italy and Malopolska Poland) and study the variability of the concentration reductions obtained with the four emission inventories in the EMEP model, considering a meteorology fixed at 2015. More details on the model, methodology and emission inventories are given in Chapter 2. Followed by the analysis of the results in Chapter 3. In Chapter 4 the conclusions are provided.

80

## 2. Methodology

Four emission inventories are used to feed the EMEP model, to understand how this input data influences the model responses. We performed the simulations for the year 2015 over Europe. More details on the model are given in the next section.

We reduced the emissions of NO<sub>x</sub>, VOCs, NH<sub>3</sub>, SO<sub>x</sub> and PPM (PM<sub>25</sub> and PM<sub>coarse</sub>) by 25% and 50% for each species separately for six cities (Brussels, Madrid, Rome, Bucharest, Berlin and Stockholm) and two regions (Malopolska, Poland and Po Valley, Italy) to study the impact on particulate matter (PM) and ozone (O<sub>3</sub>) formation. These emission reductions are theoretical and do not link with explicit and specific measures. Note that for the analysis for Malopolska, the city centre of Krakow is selected, and for the Po Valley the city centre of

90



Milan, while the emission reductions are based on the entire domain, as described in Table S1 of the Electronic Supplement (ES).

An overview of the characteristics of each domain for which the emissions are reduced is presented in Table S1 (ES). Below we present the air quality model and the emission inventories used in this study, together with the relevant indicators considered for this study.

## 2.1 The EMEP air quality model

In this study the EMEP model version rv\_34 is used, which is an off-line regional transport chemistry model (Simpson et al., 2012; <https://github.com/metno/emep-ctm>), to study the sensitivity of model responses to emission changes in Europe to emissions.

The model domain stretches from  $-15.05^{\circ}$  W to  $36.95^{\circ}$  E longitude and  $30.05^{\circ}$  N to  $71.45^{\circ}$  N latitude with a horizontal resolution of  $0.1^{\circ} \times 0.1^{\circ}$  and 20 vertical levels, with the first level around 45 m. The EMEP model uses meteorological initial conditions and lateral boundary conditions from the European Centre for Medium Range Weather Forecasting (ECMWF-IFS) for the meteorological year 2015. The temporal resolution of the meteorological input data is daily, with 3-hours timesteps. The initial and background concentrations for ozone are based on Logan (1998) climatology, as described in Simpson et al. (2003). For the other species, background/initial conditions are set within the model using functions based on observations (Simpson et al., 2003 and Fagerli et al., 2004). More detailed information on the meteorological driver, land cover, model physics and chemistry are provided in De Meij et al., (2022) and references therein.

## 2.2 Emission inventories

In this study we used the anthropogenic emissions of four emission inventories, all for the year 2015. The emission inventories are:

1. EDGAR v5.0.
2. EMEP-GNFR
3. CAMS-REG v2.2.1.
4. CAMS-REG v4.2 with condensables.

Note that, while EDGAR is completely independent from the other emission inventories, there are common features in the other three inventories. For example, emission inventories 2 and 3 share the same country totals but use different proxies to grid emissions; while emission inventories 3 and 4 only differ in terms of version from 2.2.1 to 4.2 with 4 also containing condensables in addition to 3. "Condensables" represent the fraction consisting of organic vapour able to react and/or produce condensed species when cooling.

### 2.2.1 EDGAR

The Emissions Database for Global Atmospheric Research (EDGAR) is a global inventory providing greenhouse gas and air pollutant emissions estimates for all countries over the time period 1970 till most recent years, covering



all IPCC reporting categories, with the exception of Land Use, Land Use Change and Forestry (LULUCF). It uses a bottom-up approach, i.e. using activity data and country specific emission factors based on IPCC  
130 recommendations to estimate emission quantities (Crippa et al., 2018).

For this work, we use the EDGAR 5.0 inventory (further denoted as EMEPE), that contains anthropogenic emissions for aerosol and aerosol precursor gases at 0.1 x 0.1 horizontal resolution. The inventory is available at [https://EDGAR.jrc.ec.europa.eu/dataset\\_ap50](https://EDGAR.jrc.ec.europa.eu/dataset_ap50); Janssens-Maenhout et al., 2019, Crippa et al., 2020). More information about the emission inventory is given in Thunis et al., 2021b and references therein.

135

### 2.2.2 EMEP-GNFR

The EMEP-GNFR (Gridded Nomenclature For Reporting) emissions (Mareckova et al., 2017), further denoted as EMEPG, are compiled within the “UNECE co-operative programme for monitoring and evaluation of the long-range transmission of air pollutants in Europe” (unofficially ‘European Monitoring and Evaluation Programme’,  
140 EMEP). EMEP is a scientifically based and policy driven programme under the Convention on Long-range Transboundary Air Pollution (CLRTAP) for international co-operation, that has the final aim of solving transboundary air pollution problems. More specifically, the EMEP emissions are built from officially reported data provided to CEIP (Centre of Emission Inventory and Projection, a body of EMEP) by the Convention Parties (Member States, in Europe); emissions are gap-filled with gridded TNO data from Copernicus Atmospheric  
145 Monitoring Service (CAMS) and EDGAR. The dataset consists of gridded emissions for SO<sub>x</sub>, NO<sub>x</sub>, NMVOC, NH<sub>3</sub>, CO, PM<sub>2.5</sub>, PM<sub>10</sub> and PM<sub>coarse</sub> at 0.1° x 0.1° resolution. More information on the emissions and where to download can be found in the User Guide ([https://emep-ctm.readthedocs.io/\\_/downloads/en/latest/pdf/](https://emep-ctm.readthedocs.io/_/downloads/en/latest/pdf/)) and in Mareckova et al., (2017).

### 150 2.2.3 CAMS-REG v2.2.1

The Copernicus Atmosphere Monitoring Service Regional Anthropogenic Air Pollutants (CAMS-REG-AP) emission inventory, Granier et al., 2019) covers emissions for the UNECE-Europe for the main air pollutants and greenhouse gases. Version 2.2 (further denoted as EMEPC2) and newer include a new source sector classification, namely GNFR instead of SNAP, and is an update of the TNO\_MACC, TNO\_MACC-II and TNO\_MACC-III  
155 inventories (Kuenen et al., 2014, 2021).

The CAMS-REG-AP methodology starts from the emissions reported by European countries to UNFCCC (for greenhouse gases) and to EMEP/CEIP (for air pollutants), aggregated into different combinations of sectors and fuels. Then, these emissions are gridded using ad-hoc proxies, that differ from the ones used in the EMEPG emissions. The spatial resolution of the emissions is 0.1° x 0.05°, and include CH<sub>4</sub>, NMVOC, CO, SO<sub>2</sub>, NO<sub>x</sub>,  
160 NH<sub>3</sub>, PM<sub>10</sub>, PM<sub>2.5</sub>. More information can be found in Granier et al. (2019) and Thunis et al., (2021b).

### 2.2.4 CAMS-REG v4.2 + condensables

This inventory (Kuenen et al., 2021, 2022) is an update of the previous CAMS versions for PM emissions for the residential sector. We replaced PM<sub>2.5</sub> and PM<sub>10</sub> emissions with information on the condensable part (personal



165 communication J. Kuenen, TNO, 2021), also known as REF2, further denoted as EMEPC42C. The condensables  
replace country reported PM<sub>2.5</sub> and PM<sub>10</sub> in the CAMS-REF1 emission inventory, with a bottom-up estimate  
for small combustion for all fuels (not only wood but also for fossil fuels). In countries such as Poland and Turkey,  
coal combustion in households is still an important contributor to PM. Therefore, condensables contribute not  
only to fine PM, but also to coarse PM.

170

Emissions in the four emission inventories are all given in GNFR classification. For an overview of the GNFR  
classifications we refer to Table 2 of the ES.

### 2.3 Indicators for the comparison

175 In this section we analyse the impact of the emission reduction on simulated yearly concentrations for the six  
cities and two regions. To perform this analysis, we use the potency and potential indicators as defined in Thunis  
et al. (2015a, b) based on 50% emission reduction strengths. These indicators are specifically designed to analyse  
the impact of emission reductions on concentration changes. We only recall their basic definitions here:

180 The Absolute Potential (AP) is defined as the concentration change (between the baseline and the scenario)  
divided by the reduction strength. It is expressed in µg/m<sup>3</sup>.

$$AP = \frac{C_{Scenario} - C_{Baseline}}{\alpha}$$

185

$C_{Baseline}$  represents the baseline yearly concentrations,  $C_{Scenario}$  the ‘scenario’ yearly concentrations and alpha the  
emission reduction strength, i.e.  $\alpha = 0.25$  (25% reduction),  $\alpha = 0.50$  (50% reduction), etc. All indicators  
are calculated as 95th percentiles, i.e. based on the average of all concentration values modelled in a given area  
that exceed the 95th percentile threshold. Note that the grid cells for these concentration values are selected from  
190 the baseline and kept unchanged for the scenario. The absolute potential informs on the concentration change  
projected to 100% from a given scenario.

The relative potential (RP) is obtained by dividing the absolute potential by the baseline concentration.

$$RP = \frac{C_{Scenario} - C_{Baseline}}{\alpha C_{Baseline}}$$

195

The RP provides similar information as the AP, but because it normalises the concentration change by the baseline  
concentration, it removes the impact of potential biases among baselines when different models are compared to  
each other.

200 The Potency (P) in µg/m<sup>3</sup>/(ton/day) is defined as the ratio of the concentration change by the emission change E.

$$P = \frac{C_{Scenario} - C_{Baseline}}{E_{Scenario} - E_{Baseline}}$$



205 The Potency informs on the potential concentration change per unit emission change. The normalisation by the emission change allows (at least partly) to exclude the impact of differences in the absolute levels of emissions in models when performing the comparison.

#### 2.4 Screening method statistical analysis

210 In this section, we provide a summary of the screening method which is adapted from Thunis et al. (2022). The approach aims at comparing the modelling responses from different models over a series of geographical areas. Based on gridded emissions detailed in terms of pollutants (denoted as “p”) and sectors of activity (denoted as “s”), the consistency between two modelled responses (or absolute potential - AP) is decomposed into two aspects: (1) the potency (P) and the underlying emissions (E). To do this, we decompose the ratio of the known absolute  
215 potentials of two models for each city as follows:

$$\frac{AP_{p,s}^1}{AP_{p,s}^2} = \frac{AP_{p,s}^1}{\alpha E_{p,s}^1} * \frac{\alpha E_{p,s}^1}{\alpha E_{p,s}^2} = \frac{P_{p,s}^1}{P_{p,s}^2} * \frac{E_{p,s}^1}{E_{p,s}^2} \quad (1)$$

Superscripts refer to the two models. Equation (1) is an identity where all terms are known from input quantities, i.e. the two modelled absolute potentials detailed in terms of pollutants and sectors on the left-hand side and the  
220 ratios of the potencies and emissions on the right-hand side.

For convenience, we rewrite equation (1) in logarithm form (2) considering the absolute values of the potencies only, as:

$$\log \left( \frac{AP_{p,s}^1}{AP_{p,s}^2} \right) = \log \left( \left| \frac{P_{p,s}^1}{P_{p,s}^2} \right| \right) + \log \left( \frac{E_{p,s}^1}{E_{p,s}^2} \right) \quad (2)$$

225 Which can be rewritten as equation (3) with simplified notations:

$$\widehat{AP}_{p,s} = \widehat{P}_{p,s} + \widehat{E}_{p,s} \quad (3)$$

where the hat symbol indicates that quantities are expressed as logarithmic ratios. These quantities are at the basis of the screening methodology and serve as input for the graphical representation as well. The implicit assumption  
230 is that AP1 and AP2 or P1 and P2 has the same sign. It will be the case in most cases except in a case of strong non linearities as for Ozone.

We proceed with a number of steps that help focusing on priority aspects. First, we restrict the screening only to absolute potentials that are relevant, i.e. large enough. In practice, for each city, a specific potential (p,s) needs to  
235 fulfill  $AP_{p,s} > \gamma \times \max_{city} \{AP_{p,s}\}$  to be further considered in the screening.  $\gamma$  is a user defined threshold parameter,



set to 20% in this work. Second, we flag, among the remaining potentials, only those for which differences between models are larger than a threshold,  $\beta$ , also set to 20% in this analysis. Beyond this threshold, differences are thought to be large enough to justify further checking.

240 Relation (3) is the basis of the “diamond” diagram (see Fig. 3 as an example) that provides an overview of all inconsistencies detected during the screening process. In this diagram, each inconsistent potential [p,s] is represented by a point that has emissions ( $\hat{E}$ ) as abscissa and potency as ordinate ( $\hat{P}$ ). The sum of these two terms ( $\hat{AP}$ ) is equal for points that lie on “-1” slope diagonals. At this stage it is important to note that positive differences in terms of emissions and potencies will characterize points lying on the right and top parts of the  
245 diagram, respectively. In addition, the upper right and lower left diagram areas indicate summing-up effects whereas the lower right and top left areas highlight compensating effects.

The diamond shape (in the middle of the diagram) derives from equation (3) where the  $\beta$  threshold is used to draw the inconsistency limit for each of its two terms, as well as their sum. Each [p,s] point lying outside this shape is  
250 therefore characterized by an inconsistency in terms of either E or P or/and AP, small or large according to its distance from the diamond.

In this diagram, shapes are used to differentiate sectors while colours differentiate emitted precursors. To reflect the differences in potentials (concentration change resulting from an emission reduction) of different precursors,  
255 the size of a symbol is set proportional to the maximum potential found over all precursors and all models, for each city. Finally, we use symbol filling to distinguish cases where the modelled responses change signs (filled symbol) between models (i.e. a positive vs a negative concentration change).

We also use the median concept as discussed in Thunis et al. (2023). The median is calculated from potentials  
260 obtained with the three state-of-the-art emission inventories (CAM5, EDGAR and EMEP). The proposed approach then consists in comparing each inventory with the median to identify inconsistencies (see Thunis et al. 2023 for more details). The median is not meant here to represent a more accurate model response but rather as a common benchmark to compare models to.

265



### 3. Results

In this section we first assess the level of consistency in terms of input emissions, the driving factor for potential differences, before analysing their impact in terms of concentration changes.

270

#### 3.1 Analysis of the emissions

Analysing the PPM emissions from the four emission inventories in Fig. 1, we see that all emissions compare well in general, apart from EMEPG in Bucharest (lower) and EMEPC2 in Stockholm (lower). EMEPE (red coloured) registers the highest PPM emissions for Malopolska, the Po valley, Rome and Stockholm. The differences in PPM emissions between EMEPC2 and EMEPC42C can be explained by the replacement in the EMEPC2 (REF1) inventory of country reported PM<sub>2.5</sub> and PM<sub>10</sub> emissions for residential heating by emissions that account for condensables in EMEPC42C. Condensables are emitted as gaseous compounds, that immediately condense to form organic aerosols. They lead to overall higher PM emissions in EMEPC42C. Significant changes in PM<sub>2.5</sub> emission quantities due to the presence of condensables are found for several countries, like Spain, Italy and Romania, while differences are smaller for Germany and France (Kuenen et al., 2022). This corroborates the higher PPM emissions in EMEPC42C than EMEPC2 for the Po valley, Rome, Madrid and Stockholm found in this study. The emission quantities for each location, pollutant (PPM, NO<sub>x</sub>, SO<sub>x</sub>, NH<sub>3</sub>, VOC) and inventory are given in Table S3 of the Electronic Supplement of this study.

275

280

285

Furthermore, Kuenen et al., (2022) showed that the emission differences between EMEPC2 and EMEPC42C can be explained by the different methodologies and recalculation of the officially reported emissions. Also, each year, an update is processed of the past country's reported emissions based on latest information of activity data or emission factors (EFs). This helps to explain the differences between the emission inventories and reported years.

290

Kuenen et al., (2022) also showed that in general, for Europe, NMVOC, NH<sub>3</sub>, PPM<sub>10</sub>, PPM<sub>2.5</sub>, NO<sub>x</sub> and SO<sub>2</sub> emissions are higher in EDGAR than in CAMS42, with larger differences for non-EU countries. This could be explained by the fact that EDGAR uses a bottom-up methodology instead of the reported country totals, which has been shown to have higher uncertainties (Cheewaphongphan et al., 2019).

295

In our study, we compare the emission densities for smaller areas, but we find similar differences, i.e. EDGAR registers higher emissions for the above-mentioned pollutants for the eight areas considered in our study, apart from yearly NO<sub>x</sub> emissions for Bucharest, Madrid, Malopolska, Rome and Po Valley, where the emission densities are similar to the other three emission inventories. Also, there are substantial differences in PPM emissions for Bucharest between EMEPG (3.1 mg/m<sup>2</sup>/day) and the other three inventories, 7.6 mg/m<sup>2</sup>/day for

300



EMEPE, 8.0 mg/m<sup>2</sup>/day for EMEPC2 and 8.2 mg/m<sup>2</sup>/day for EMEPC42C, which clearly impact the calculated PM10 concentrations, as will be further discussed in the next section.

305 Overall, SO<sub>x</sub>, NH<sub>3</sub> and VOC by EMEPG and the two CAMS inventories agree well, while EDGAR generally shows higher emission densities for these pollutants except for Bucharest and Po Valley for VOC and NH<sub>3</sub> for Madrid and Bucharest.

More details on the explanation regarding the differences between EMEPC2, EMEPC42C and EDGAR are described in Kuenen et al., (2022). At the urban scale, Thunis et al. (2021b) showed that for some sectors and  
310 pollutants, the EDGAR emissions were significantly larger than other inventories. This is the case for the SO<sub>2</sub> emissions from the industrial sector because of differences in terms of country totals but also in terms of spatial proxies used.

More in-depth analysis and the explanation on the underlying differences in air pollutants between the emission  
315 inventories – as used in this study - is given in Thunis et al. (2022) They identify the largest inconsistencies between the emission inventories in terms of pollutant and sector for 150 cities in Europe and show that the difference for some air pollutants between emission inventories can be as large as a factor of 100 or more. They explain that the underlying reason for these discrepancies is related to the differences in spatial proxies, country totals (i.e. differences in urban area share) and country sectoral share (e.g. industry, residential, power plants).

320

### 3.2 Variability of PM10 base-case concentrations

Aerosol can either be produced by ejection into the atmosphere, or by physical and chemical processes within the atmosphere, called primary and secondary aerosol production respectively. Secondary aerosol formation is more  
325 complex, because of the chemical and physical processes involved, such as sulphate aerosol formation from SO<sub>2</sub> or nitrate aerosol formation from NO<sub>x</sub> or organic aerosol formation from VOCs.

Sulphate is produced by chemical reactions in the atmosphere from gaseous precursors (combustion of sulphur containing fuels and industrial processes). The oxidation of SO<sub>2</sub> in cloud liquid water by H<sub>2</sub>O<sub>2</sub> is very fast and is an important source (more than half) of all the sulphate aerosol formation (De Meij A. 2009b and references  
330 herein). The sulphate can react with ammonia to form the ammonium sulphate aerosol. The production of nitrate aerosol can be understood from the NO<sub>x</sub> and NH<sub>3</sub> precursor emissions. NO<sub>x</sub> is emitted mainly via combustion for energy production and by traffic. NH<sub>3</sub> is emitted from agricultural activities. If sufficient ammonia is available to neutralize all sulphate, the residual amount of ammonia can neutralize nitric acid to form the ammonium nitrate aerosol.

335 Yearly averaged PM10 concentrations from EMEPE are in general higher than with the other emission inventories, except for Brussels, Madrid and Stockholm (Fig. 2). We have seen in section 3.1 that for some locations PPM, SO<sub>x</sub>, NH<sub>3</sub> or NMVOC emissions from EMEPE are higher than the other three inventories. However, differences in emissions do not lead to important differences in terms of PM10 concentrations.



340 For Malopolska we find that PM10 values by EMEPC42C are higher than EMEPC2 and EMEPG due to the  
inclusion of condensables for residential heating. Note that inclusion of condensables leads to larger differences  
over the eastern part of Europe.

Interesting to mention is the large difference in PM10 concentrations for Bucharest between EMEPG and the other  
three inventories (EMEPG lower), which can be explained, at least partly, by the differences in PPM emissions,  
345 as mentioned in Section 3.1.

### 3.3 Analysis of potentials and potencies for PM10

Fig. 3 represents the impact on calculated PM10 concentrations of emission reduction of NH<sub>3</sub>, VOC, NO<sub>x</sub>, PPM  
350 and SO<sub>x</sub> for the different locations. The plots show the potency on the y-axis, the emissions on the x-axis and the  
potential along descending diagonal (indicated with dashed lines). The diamond shape (delineated by black bold  
lines), indicate that the differences in emissions, potencies and potentials between a given model and the median  
are below 20%, where the Median is calculated from three emission inventories: EMEPE, EMEPC2 and EMEPG.  
The 'fac2' and 'fac5' lines indicate a factor of two and five as compared to the median, respectively. The  
355 consistency indicator (top right) provides information on the percentage of pollutant/sector (p,s) couples that fall  
within the diamond shape, e.g. in the case of EMEPC42C, 50% of the (p,s) couples show differences with the  
median estimate that remain below 20%. Below we analyse the results per precursor.

#### 3.3.1 PPM

360 EMEPG calculates much higher potentials for PM10 in Stockholm, due to an overestimation of the PPM potency  
by a factor ~2, see Fig. 3b. For Bucharest a much lower potential for PM10 is found, which can be explained by  
the underestimation (around a factor 2) of the PPM emissions. Also, EMEPC2 displays lower PPM emissions for  
Stockholm (Fig. 3c), but these lower emissions are compensated by higher potencies (factor ~2 higher), leading  
to similar PM10 potentials as for the other inventories. For Berlin, the EMEPC2 PPM potency is more than a  
365 factor 2 lower, leading to underestimation in terms of potential of a factor ~2, despite a slight overestimation of  
the emissions. Because PPM does not undergo chemical reactions, we expect a relatively linear relationship  
between emissions and concentrations. In other words, we expect emissions and potentials to be correlated (e.g.  
Bucharest for EMEPG). In some instances, this is however not the case (e.g. Stockholm for EMEPG and  
EMEPC42C). These differences can partly be explained by the sector allocation of the PPM emissions in the four  
370 inventories, as shown in Fig. 4. EMEPE assigns much larger PPM emissions in sector 2 (Industry), while EMEPG  
has larger PPM emissions in sector 6 (road transport). This is important as emissions are distributed vertically in  
a different way depending on the sector. Industrial emissions, mainly emitted by stacks at higher levels travel over  
larger distances and will have less impact on surface concentrations locally than emissions emitted at ground such  
as road transport. This explains the much higher potencies in EMEPG. It also stresses the importance of the  
375 sectorial repartition of the emissions, especially for PPM that generally shows the largest potencies.



Another reason is for these differences is the spatial distribution of the emissions which differ from one inventory to the other (see supplementary material Fig. S1). Indeed, we see differences in the geographical distribution of the PPM<sub>2.5</sub> emissions between the four inventories for the different locations.

380 As mentioned before, EMEPC42C includes condensables leading to larger PM<sub>10</sub> potentials than EMEPC2. Despite the overall increase of PPM emissions caused by the inclusion of condensables in EMEPC42C, emissions remain lower than the median in cities like Stockholm (red circle in Fig. 3d). For Malopolska the potential is larger for EMEPE and EMEPC42C (see also Fig. S2 ES), partly caused by larger emissions.

385 Apart from the vertical and spatial distribution of the emissions, another reason for differences in potentials might be related to the fact that the location of the P95 values cells where the concentration changes are calculated differ for each model, as shown in Fig.5. More specifically, the P95 values might be positioned at different locations in the 4 Base Cases (see Fig. 5 shaded grid cells).

390 PM<sub>10</sub> includes not only primary particles, but also secondary particles. Secondary particles are formed by gases reacting (such as NO<sub>x</sub>, VOC and SO<sub>x</sub>) and condensing (gas to particle conversion) onto pre-existing particles or by nucleation. In the next section we present an evaluation of the impact of the reduction of the aerosol secondary precursors on calculated PM<sub>10</sub> concentrations.

### 3.3.2 NO<sub>x</sub>

395 Compared to other precursors, NO<sub>x</sub> shows a good agreement among models with a couple of inconsistencies identified in the Po Valley for EMEPE and EMEPC42C, where the potencies are slightly larger than the 20% threshold around the median. This good agreement can be explained by the fact that NO<sub>x</sub> emissions originate in great part from the transport sector, a sector for which the spatial proxies (for the spatial and sectorial disaggregation) are generally well described and harmonised among inventories (Trombetti et al. 2018). In addition, NO<sub>x</sub> sources are mostly diffuse (as opposed to point sources) and less subject to localised hot-spot differences.

### 3.3.3 SO<sub>x</sub>

405 For Stockholm large differences are found in EMEPE potentials when compared to the median (Fig.3a, indicated by red coloured rectangular box). The explanation for this is a strong overestimation of the SO<sub>x</sub> emissions (factor ~10, Fig. 1c), which is partly compensated by an underestimation of the potency (factor ~2). For BUC and BRU, we see that higher SO<sub>x</sub> emissions (factor ~2) by EMEPE are compensated by lower potencies, which lead to overall similar potentials.

410 Higher SO<sub>x</sub> emissions in EMEPE (Fig. 1c and Fig3.a) lead to larger potentials (see also Fig. S2 – S4), indicating that a reduction of SO<sub>x</sub> in EMEPE lead to a higher reduction of PM. The differences are smaller for Bucharest and Malopolska, probably because of differences in terms of chemical regime that favour more efficient reactions with other precursors. Hence, reducing SO<sub>x</sub> emissions in EMEPE has a larger impact on PM<sub>10</sub> concentrations



via the chemical reactions that lead to the formation of ammonium sulphate aerosol as described in (De Meij et al., 2009c).

415

### 3.3.4 NH<sub>3</sub>

With the exception of EMEPG, all models show a problem for NH<sub>3</sub> in the Malopolska region. EMEPE shows higher emissions (factor ~2) than the ensemble, but these higher emissions are compensated by lower potencies, which lead to overall similar potentials. EMEPC and EMEPC42 both show larger emissions too (although to a lesser extent than EMEPE) and lower potencies, leading to relatively similar potentials (green diamond symbols in Fig. 3). Note that given the reduced NH<sub>3</sub> emissions in urban areas, these emissions do not lead to important potentials in many cities, hence they do not appear in the diagrams.

420

### 3.3.5 VOC

For VOC potentials are generally too low (lower than the 20% threshold detailed in Section 2.4) to appear in the figures, apart from the Po Valley where EMEPC shows a small inconsistency with respect to the median (orange squares in Fig. 3).

425

From the analysis of these different precursors, PPM appears to be the precursor leading to the major differences in terms of potentials, i.e. in terms of concentration change responses that are of direct relevance when designing air quality plans (Fig. S5). Although simpler to manage because of their linearity, they deserve more attention given their important variability (among models) and importance in terms of final concentrations.

430

To understand better the sensitivity of PM<sub>10</sub> formation to NO<sub>x</sub>, SO<sub>x</sub>, or NH<sub>3</sub> reductions, we analyse the ratios between these precursors across inventories.

435

Table 1a shows the ratios between Base Case domain averaged SO<sub>x</sub> and NO<sub>x</sub> emission densities. For example, the minimum ratio is around 0.06, indicating that there are around 16 times more NO<sub>x</sub> (11.5 mg/m<sup>2</sup>/day) than SO<sub>x</sub> emissions (0.74 mg/m<sup>2</sup>/day) emissions in Rome for EMEPG. Table 1b shows on the other hand that the corresponding potency ratios are inverted, with much larger efficiencies when reducing SO<sub>x</sub> than NO<sub>x</sub> emissions.

440

The same is true in most cities. This can be explained by the fact that NO<sub>x</sub> has to compete with NH<sub>3</sub> to form PM whereas SO<sub>x</sub> emission reductions directly lead to PM changes. While this behaviour is quite general, there is a large variability in its magnitude. In some cities like Brussels, negative ratios appear caused by concentration increases when NO<sub>x</sub> emissions are reduced. This corroborates the findings by Clappier et al., (2021) who found that reducing SO<sub>2</sub> emissions where abundant is always efficient and relatively linear, as shown also in the next section on non-linearities.

445

A similar analysis can be performed with NO<sub>x</sub> to NH<sub>3</sub> ratios. NO<sub>x</sub> to NH<sub>3</sub> contribute to the formation of ammonium nitrate aerosol, via the reactions NO<sub>2</sub> + OH → HNO<sub>3</sub>, that reacts (when there is sufficient ammonia available to neutralize all sulphate) with NH<sub>3</sub> to form NH<sub>4</sub>NO<sub>3</sub> aerosol, a fraction of PM<sub>10</sub>. Details on the

450



chemical pathways can be found in Thunis et al., (2021a). As an example, the emission ratio for Rome by EMEPE is 3.3, while the corresponding numbers are 4.9, 5.4 and 4.8 for EMEPC, EMEPC42C and EMEPG, respectively. While NO<sub>x</sub> emissions in the four inventories are similar, EMEPE contains almost a factor 2 more NH<sub>3</sub> emissions, resulting in formation processes being more ‘NO<sub>x</sub>-sensitive’ in Rome. In other words, reducing NO<sub>x</sub> in EMEPE leads to larger impact on PM<sub>10</sub> concentrations.

### 3.4 Non-linearities

Non-linearity in PM responses to emission changes often results from changes in chemical regimes where the formation process is limited by a different species.

Analysing the absolute potentials ratio (50% vs. 25%) in Tables 2 to 6 provides information on the (non-)linearity of the relationship between emission and concentration changes. If the ratio is close to 1.00, then there is linear correlation between the two. Departure from 1 indicates non-linearity. We only show the ratios which are 3% or higher when compared to the 50% potential for PPM in order to highlight the most relevant ratios.

For primary PM (PM<sub>2.5</sub> and PM<sub>coarse</sub>) we get a linear relationship as expected, see Table 5. The reason for this is that primary emissions only affect the primary part of the aerosol formation and do not undergo chemical reactions.

For NO<sub>x</sub> (Table 2) the behaviour is generally non-linear with ratios larger than 1.00, indicating a larger efficiency for more important emission reductions. For example, EMEPE indicates 1.18 in Rome, indicating that PM<sub>10</sub> concentrations would be 18% more reduced between 25 and 50% than between 0 and 25%. This might be explained by a change of chemical regime from a NH<sub>3</sub>-limited regime (when NO<sub>x</sub> is more abundant and less efficient) to a NO<sub>x</sub>-limited regime (NO<sub>x</sub> is less abundant and more efficient) as emissions are reduced further.

Note the importance of averaging processes on the indicator value. Based on 95-percentile locations, the ratio for Bucharest with EMEPG is 1.18 whereas for domain-averaged values the ratio becomes 1.08 indicating closer to linear relationships. Indicators based on averaged values tend to report more linear relationships as shown by Thunis et al., (2021c).

For VOC (Table 3) and SO<sub>x</sub> (not shown, as the ratios compared to PPM are less than 3%) we find that ratios remain very close to 1.00.

NH<sub>3</sub> shows significant non-linearity although less important than for NO<sub>x</sub> with ratios larger than 1 (Table 4). The same explanations as for NO<sub>x</sub> can be used to explain the larger efficiency of emission reductions when these become more important.

Finally, a similar ratio can be constructed for emission reductions that include all species together (SO<sub>x</sub>, NO<sub>x</sub>, VOC, NH<sub>3</sub>, PM<sub>2.5</sub> and PM<sub>coarse</sub>). The results generally indicate a linear behaviour mainly because of dilution effects (NO<sub>x</sub> non-linearities are diluted by other emitted species), with the exception of EMEPG in Berlin and Malopolska. For these two locations, the explanation lies in the much lower PPM emissions (linear) and larger NO<sub>x</sub> emissions (non-linear).



490

### 3.5 Variability of ozone base-case concentrations

Ozone is chemically formed by the oxidation process of volatile organic compounds (VOCs) in the presence of NO<sub>x</sub> (NO + NO<sub>2</sub>) and its formation is driven by the sunlight intensity. At the same time, NO<sub>x</sub> also works as an ozone sink through NO<sub>x</sub> titration (NO+O<sub>3</sub>→NO<sub>2</sub>+O<sub>2</sub>) that occurs during the night and wintertime, i.e. less photolysis reactions of NO<sub>2</sub> (Jhun et al., 2015) and O<sub>3</sub> is removed by NO emissions from road traffic in city centres (Sharma et al.,2016).

Fig. 6 shows that yearly averaged O<sub>3</sub> concentrations are very similar.

500

### 3.6 Analysis of potentials and potencies for O<sub>3</sub>

In Fig. 7 we analyse the impact of the reduction of NO<sub>x</sub> and VOC on calculated O<sub>3</sub> concentrations for the different locations.

The production of O<sub>3</sub> depends on the availability of NO<sub>x</sub> and VOCs, which are emitted mostly from sectors such as industry and road transport. For that reason, only NO<sub>x</sub> and VOC appear in Fig. 7, except for NH<sub>3</sub> for EMEPE. The latter can be explained by the fact that NH<sub>3</sub> contributes to the formation of secondary aerosol and decreases the acidity of the aerosols. The aerosol pH plays an important role in the reactive uptake and release of gases, which can affect ozone chemistry (Poizzer et al., 2017). This NH<sub>3</sub> impact also exists for the other inventories but is lower than the 20% threshold and therefore does not appear in the diamond plots.

510

#### 3.6.1 VOC

With the exception of EMEPC2, all models show some differences with the median for VOC (Fig. 7). In Maloposka, Stockholm and Berlin, EMEPE emissions are a factor ~2 higher than the median value. While in the first location, the lower potencies compensate for these emission differences, leading to similar potentials, this is not the case for the two latter cities, where similar potencies lead to larger potential. For EMEPG, only Bucharest shows differences with lower emissions and higher potencies, leading to similar potentials. It is interesting to note the large differences between EMEPC2 and EMEPC42C. While the addition of condensable in EMEPC42C does not impact O<sub>3</sub> formation, other changes included in version EMEPC42C have significant impacts. While NO<sub>x</sub> responses dominate in most cases in EMEPC2, this is not the case in EMEPC42C where VOC responses become important for many cities. Differences with the median are mostly caused by potency rather than by emission differences. This is an interesting information that a change of version can lead to very important changes in model responses despite similar absolute O<sub>3</sub> levels.

520

Note that VOC appears systematically as an important impact (i.e. visible in the diagram) for Malopolska and Po Valley, whereas this is not the case systematically for the other locations. The reason is that for these two regions, emissions are reduced over larger areas, leading to larger impacts. More details on the potentials and potencies for the different locations can be found in the supplement material Fig. S6 – S8.

525



### 3.6.2 NO<sub>x</sub>

530 NO<sub>x</sub> shows generally larger impacts than VOC (see supplementary material Fig. S9), leading to NO<sub>x</sub> symbols  
being visible on each diagram for every city and regions. While for PM<sub>10</sub>, NO<sub>x</sub> responses were shown in the  
previous section to be consistent among models; this is not the case for O<sub>3</sub>. Potential differences originate mostly  
from differences in potencies while emissions remain relatively similar among inventories. The largest differences  
535 occur for Bucharest (EMEPEG), Malopolska and the Po valley (EMEPC42C) with much larger potency estimates  
than the median, indicating that these regions are more sensitive to NO<sub>x</sub> reduction than for other inventories.  
However, opposite trends also occur as in Berlin for EMEPC2 and EMEPC42C. It is also interesting to note that  
in some cities like Brussels, differences in model versions (EMEPC42C vs. EMEPC2) significantly affects the  
NO<sub>x</sub> responses (as already noted for VOC).

540 In Malopolska, EMEPE and EMEPC42C show a change of sign in terms of responses. In such cases, NO<sub>x</sub>  
reductions lead to an O<sub>3</sub> increase whereas the median shows an opposite behaviour.

The highest consistency (84%) with the ensemble is found for EMEPEG, meaning that 84% of the relevant impacts  
(delta concentrations) are within the 20% limit, indicating that EMEPEG is often picked as the median. On the  
545 other hand, EMEPC42C and EMEPE show the lowest consistency number. It is interesting to note the large  
difference between the two versions of the same inventory (60 vs. 35% for EMEPC2 and EMEPC42C,  
respectively).

550 Similarly to PM<sub>10</sub>, some of the differences are partly explained by the location of the P95 values that are not  
similar for the four inventories, as shown in Fig.8, where EMEPE locations differ from all others (shaded grid  
cells).

To understand better the impact of NO<sub>x</sub> and VOC reductions on the production or loss of O<sub>3</sub>, and the  
interconnections between the two, we analyse the VOC/NO<sub>x</sub> for the different inventories in Table 7a. For  
555 Malopolska, Bucharest or Brussels, the VOC/NO<sub>x</sub> emission ratio for EMEPE is twice larger than the others. This  
reflects in the EMEPEG diagram where these cities show clear inconsistencies. The larger amount of VOC in these  
cities does not impact significantly the potencies (Table 7b). While NO<sub>x</sub> potencies are mostly positive, indicating  
an increase of the O<sub>3</sub> concentrations over the urban areas, VOC potencies are always negative, indicating lower  
O<sub>3</sub> concentrations when reducing VOC emissions. Differences in VOC/NO<sub>x</sub> ratios might lead to changes of  
chemical regime, that explain some of the differences in the potentials.

560 The differences in VOC/NO<sub>x</sub> ratios between the four emission inventories highlight the importance of the  
accuracy of emission inventories, which could strongly impact the chemical regime (i.e. NO<sub>x</sub>-limited or VOC-  
limited). Even moderate perturbations in NO<sub>x</sub> or VOC emissions could change the chemical regime of O<sub>3</sub>  
formation (Xiao et al. 2010).

565



### 3.7 Non-linearities

570 Previous studies (Cohan et al. 2005, Xiao et al., 2010) have shown that the formation of ozone is more sensitive to large reductions of NO<sub>x</sub> that depart from a linear emission scaling. To this end, we show in Table 8 and 9 the ratio between absolute potentials (at 50% and 25%) for 95P, which help to assess the level of non-linearity of the atmospheric reactions that involve gaseous precursors NO<sub>x</sub>, and VOCs in the formation of ozone. Table 8 shows large non-linearities when NO<sub>x</sub> emissions are reduced. A number larger than 1 indicates that more O<sub>3</sub> is reduced for NO<sub>x</sub> emission reductions between 25 and 50% than between 0 and 25%. For Malopolska, we find a large ratio for EMEPE (12.03) because it is based on small values (-0.325 vs. -0.027).  
575 Ratios are generally lower than one, with the clear exception in the Po Valley. This must be put in relation with the fact that the Po valley is the only place where potencies are negative (see Table 7b), indicating a different chemical regime (O<sub>3</sub> formation) than in other locations (O<sub>3</sub> titration). This is explained by the fact that the Po Valley domain includes sub-urban and background areas where O<sub>3</sub> formation takes place. For VOC the ratios are close to 1.00 indicating a linear behavior (Table 9). This corroborates previous studies  
580 (Xiao et al., 2010). Reducing NO<sub>x</sub> and VOC emissions together (Table 10) also shows some non-linear behaviour that originates from the NO<sub>x</sub> side. This corroborates the findings of Xiao et al., 2010, Xing et al., 2017.

585



#### 4. Concluding remarks

590 In this work, we assessed how emissions impact the responses on air quality concentrations when emission  
reductions are applied. The impact of emission reductions based on four emission inventories (EDGAR 5.0,  
EMEPG, CAMS version 2.2.1 and CAMS version 4.2 + condensables) has been investigated for PM10 and O3 in  
eight cities/regions in Europe. We assessed the model's variability in terms of model responses to emission  
changes with the support of specific indicators (potentials and potencies) and used a screening method adapted  
600 from Thunis et al. (2022) to identify the main inconsistencies among model responses. A median value has been  
constructed to serve as reference for the comparisons.

Our study reveals that the impact of reducing aerosol (precursors), such as PPM, NOx, SO2, NH3, VOCs result  
in different potentials and potencies, differences that are mainly explained by differences in emission quantities,  
differences in their spatial distributions as well as in their sector allocation. The main findings are the following:

600

- In general, the variability among models is larger for concentration changes (potentials) than for absolute concentrations. This is true for both PM10 and O3.
- Emission densities at each location for all precursors are quite consistent apart from EDGAR which generally show larger urban scale emissions.
- 605 • Similar emissions can however hide large variations in sectorial allocation. Our results stress the importance of the sectorial repartition of the emissions, given their different vertical distribution (emissions in the industrial sector are emitted at higher levels and have less impact on surface concentration) especially PPM. This sectorial allocation can lead to large impacts on potency. For similar reasons, higher emission do not necessarily lead to higher potencies. At the local scale, it is therefore important to further work on the modelling of PPM and on the estimate of the underlying emissions.
- 610 • PPM appears to be the precursor leading to the major differences in terms of potentials, i.e. in terms of PM10 concentration changes. This is of direct relevance for designing air quality plans. Although simpler to manage because of their linearity, they would deserve more attention at the local scale given their importance in terms of final concentrations and their large variability (among models).
- 615 • For O3, NOx emission reductions are the most efficient, likely because of the urban focus of this work and the abundance of NOx emission in this type of areas.
- In terms of non-linear behavior, the relationship between emission reduction and PM10 concentration change shows the largest non-linearity for NOx and in a lesser extend for NH3 whereas it remains mostly linear for the other precursors (VOC, SOx and PPM).
- 620 • In terms of non-linear behaviour, the relationship between emission reduction and O3 concentration change shows the largest non-linearity for NOx (concentration increase) and a quasi linear behaviour for VOC (concentration decrease).



- 625 • Potencies and potentials can show differences that are as large between inventories (EMEPC2 vs EMEPG) than between inventory versions (EMEPC2 vs. EMEPC42C). This is the case for example in Brussels for the NO<sub>x</sub> responses on PM<sub>10</sub> concentrations.
- Precursor emission ratios (e.g. VOC/NO<sub>x</sub> for ozone or NO<sub>x</sub>/NH<sub>3</sub> for PM<sub>10</sub>) show important differences among emission inventories. This emphasizes the importance of the accuracy of emission estimates since these differences can lead to changes of chemical regimes, directly affecting the responses of O<sub>3</sub> or PM<sub>10</sub> concentrations to emission reductions.
- 630 • It is also important to understand that the choice of the indicator used in a given analysis (for example mean or percentile values) can lead to different outcomes. It is therefore important to assess the variability of the results around the choice of the indicator to avoid misleading interpretations of the results.

#### 635 **Code availability**

The source code of the screening method of the statistical analysis can be found here:  
<https://doi.org/10.5281/zenodo.8082531>

#### **Data availability**

The emission data can be downloaded here: <https://eccad.sedoo.fr/>

640

#### **Author contributions**

AdM and PT wrote the manuscript draft; AdM, PT and CC produced the data; AdM, PT and CC analyzed the data; EP and BB reviewed and edited the manuscript.

#### 645 **Competing interests**

The authors declare that they have no conflict of interest.

#### **Acknowledgment ECCAD**

650 The authors would like to thank Emissions of atmospheric Compounds and Compilation of Ancillary Data (ECCAD) system (<https://eccad.aeris-data.fr>) for archiving and distribution of the emission inventories.



655 **References**

Cheewaphongphan, P., Chatani, S., Saigusa, N.: Exploring Gaps between Bottom-Up and Top-Down Emission Estimates Based on Uncertainties in Multiple Emission Inventories: A Case Study on CH<sub>4</sub> Emissions in China. *Sustainability*, 11, 2054, <https://doi.org/10.3390/su11072054>, 2019.

660

Clappier, A., Thunis, P., Beekmann, M., Putaud, J.P., De Meij, A.: Impact of SO<sub>x</sub>, NO<sub>x</sub> and NH<sub>3</sub> emission reductions on PM<sub>2.5</sub> concentrations across Europe: Hints for future measure development, *Env. Int.*, Vol. 156, ISSN 0160-4120, <https://doi.org/10.1016/j.envint.2021.106699>, 2021.

665

Cohan, D. S., Hakami, A., Hu, Y. T., Russell, A. G.: Nonlinear response of ozone to emissions: Source apportionment and sensitivity analysis, *Env. Sci. Tech.*, 39(17), 6739–6748, doi:10.1021/es048664m, 2005.

670

Crippa, M., Guizzardi, D., Muntean, M., Schaaf, E., Dentener, F., van Aardenne, J. A., Monni, S., Doering, U., Olivier, J. G. J., Pagliari, V., and Janssens-Maenhout, G.: Gridded emissions of air pollutants for the period 1970–2012 within EDGAR v4.3.2, *Earth Syst. Sci. Data*, 10, 1987–2013, <https://doi.org/10.5194/essd-10-1987-2018>, 2018.

675

Crippa, M., Solazzo, E., Huang, G., Guizzardi, D., Koffi, E., Muntean, M., Schieberle, C., Friedrich, R. and Janssens-Maenhout, G.: High resolution temporal profiles in the Emissions Database for Global Atmospheric Research, *Sci Data* 7, 121, 2020.

680

De Meij, A., S. Wagner, N. Gobron, P. Thunis, C. Cuvelier, F. Dentener, M. Schaap: Model evaluation and scale issues in chemical and optical aerosol properties over the greater Milan area (Italy), for June 2001, *Atmos. Res.* 85, 243-267, 2007.

685

De Meij, A., Gzella, A., Cuvelier, C., Thunis, P., Bessagnet, B., Vinuesa, J. F., Menut, L., Kelder, H. M.: The impact of MM5 and WRF meteorology over complex terrain on CHIMERE model calculations, *Atmos. Chem. Phys.*, 9, 6611–6632, <https://doi.org/10.5194/acp-9-6611-2009>, 2009a.

690

PhD thesis, De Meij, A.: Uncertainties in modelling the spatial and temporal variations in aerosol concentrations, Eindhoven University of Technology, the Netherlands, <http://alexandria.tue.nl/extra2/200911524.pdf>, 2009b.

De Meij, A., Thunis, P., Bessagnet, B., Cuvelier, C.: The sensitivity of the CHIMERE model to emissions reduction scenarios on air quality in Northern Italy, *Atmos. Env.* Vol. 43, Issue 11, Pages 1897-1907, April 2009c.

695

De Meij, A., Bossioli, E., Vinuesa, J.F., Penard, C., Price, I.: The effect of SRTM and Corine Land Cover on calculated gas and PM<sub>10</sub> concentrations in WRF-Chem, *Atmos. Env.* Vol. 101, Pages 177–193, January 2015.



- 695 De Meij, A., Zittis, G. & Christoudias, T.: On the uncertainties introduced by land cover data in high-resolution regional simulations, *Meteorol. Atmos. Phys.*, <https://doi.org/10.1007/s00703-018-0632-3>; <https://rdcu.be/38pt>, 2018.
- De Meij, A., Astorga, C., Thunis, P., Crippa, M., Guizzardi, D., Pisoni, E., Valverde, V., Suarez-Bertoa, R., Oreggioni, G.D., Mahiques, O., Franco, V.: Modelling the Impact of the Introduction of the EURO 6d-TEMP/6d Regulation for Light-Duty Vehicles on EU Air Quality. *Appl. Sci.*, 12, 4257. <https://doi.org/10.3390/app12094257>, 2022.
- 700 European Commission: Proposal for a DIRECTIVE OF THE EUROPEAN PARLIAMENT AND OF THE COUNCIL on ambient air quality and cleaner air for Europe, COM (2022) 542 final, 2022/0347 (COD), October 2022.
- 705 European Environment Agency: Air quality in Europe — 2020 report, EEA report N°09/2020, <https://www.eea.europa.eu/publications/air-quality-in-europe-2020-report>, 2020.
- 710 Fagerli, H., Simpson, D., Tsyro, S.: Unified EMEP model: Updates. In EMEP Status Report 1/2004, Transboundary acidification, eutrophication and ground level ozone in Europe. Status Report 1/2004, pages 11–18. The Norwegian Meteorological Institute, Oslo, Norway, 2004.
- Georgiou, G.K., Kushta, J., Christoudias, T., Proestos, Y., Lelieveld, J.: Air quality modelling over the eastern Mediterranean: seasonal sensitivity to anthropogenic emissions, *Atmos. Env.*, 222, 2020.
- 715 Granier, C., Darras, S., Denier van der Gon, H., Doubalova, J., Elguindi, N., Galle, B., Gauss, M., Guevara, M., Jalkanen, J.-P., Kuenen, J., Liousse, C., Quack, B., Simpson, D., Sindelarova, K.: The Copernicus Atmosphere Monitoring Service Global and Regional Emissions (April 2019 Version), Copernicus Atmosphere Monitoring Service, 10.24380/d0bn-kx16 (CAMS) report, [https://atmosphere.copernicus.eu/sites/default/files/2019-06/cams\\_emissions\\_general\\_document\\_apr2019\\_v7.pdf](https://atmosphere.copernicus.eu/sites/default/files/2019-06/cams_emissions_general_document_apr2019_v7.pdf), 2019.
- Janssens-Maenhout G., et. al: EDGAR v4.3.2 Global Atlas of the three major greenhouse gas emissions for the period 1970–2012, *Earth Syst. Sci. Data*, 11, 959–1002, 2019.
- 725 Jhun, I., Coull, B.A., Zanobetti, A., Koutrakis, P: The impact of nitrogen oxides concentration decreases on ozone trends in the USA, *Air Qual. Atmos. Health.*, 283-292. doi:10.1007/s11869-014-0279-2, 2015.
- 730 Kuenen, J. J. P., Visschedijk, A. J. H., Jozwicka, M., Denier van der Gon, H. A. C.: TNO-MACC\_II emission inventory; a multi-year (2003–2009) consistent high-resolution European emission inventory for air quality modelling, *Atmos. Chem. Phys.*, 14, 10963–10976, <https://doi.org/10.5194/acp-14-10963-2014>, 2014.



- 735 Kuenen, J., Dellaert, S., Visschedijk, A., Jalkanen, J.-P., Super, I., Denier van der Gon, H.: Copernicus Atmosphere Monitoring Service regional emissions version 4.2 (CAM5-REG-v4.2) Copernicus Atmosphere Monitoring Service, ECCAD, doi:10.24380/0vzb-a387, 2021.
- 740 Kuenen, J., Dellaert, S., Visschedijk, A., Jalkanen, J.-P., Super, I., Denier van der Gon, H.: CAM5-REG-v4: a state-of-the-art high-resolution European emission inventory for air quality modelling, *Earth Syst. Sci. Data*, 14, 491–515, <https://doi.org/10.5194/essd-14-491-2022>, 2022.
- Logan, J. A.: An analysis of ozonesonde data for the troposphere: Recommendations for testing 3-D models and development of a gridded climatology for tropospheric ozone, *J. Geophys. Res.*, 10, 16115–16149, 1998.
- 745 Mareckova, K., Pinterits, M., Ullrich, B., Wankmueller, R., Mandl, N., Review of emission data reported under the LRTAP Convention and NEC Directive Centre Emission Inventories Project., 10.1029/2009JD011823, 2017.
- Pozzer, A., Tsimpidi, A. P., Karydis, V. A., de Meij, A., Lelieveld, J.: Impact of agricultural emission reductions on fine-particulate matter and public health, *Atmos. Chem. Phys.*, 17, 12813–12826, <https://doi.org/10.5194/acp-17-12813-2017>, 2017.
- 750 Sharma, S., Sharma, S., Khare, M., Kwatra, S.: Statistical behavior of ozone in urban environment, *Sustain. Env. Res.*, Vol. 26, Issue 3, ISSN 2468-2039, <https://doi.org/10.1016/j.serj.2016.04.006>, 2016.
- 755 Simpson, D., Fagerli, H., Jonson, J., Tsyro, S., Wind, P., Tuovinen, J.-P.: The EMEP Unified Eulerian Model. Model Description, EMEP MSC-W Report 1/2003, The Norwegian Meteorological Institute, Oslo, Norway, 2003.
- Simpson, D., Benedictow, A., Berge, H., Bergström, R., Emberson, L.D., Fagerli, H., Flechard, C.R., Hayman, G.D., Gauss, M., Jonson, J.E., Jenkin, M.E., Nyíri, A., Richter, C., Semeena, V.S., Tsyro, S., Tuovinen, J.-P., Valdebenito, Á., Wind, P.: The EMEP MSC-W chemical transport model – technical description. *Atmos. Chem. Phys.* 12, 7825–7865. <https://doi.org/10.5194/acp-12-7825-2012>, 2012.
- 760 Thunis, P., Clappier, A., Pisoni, E., Degraeuwe, B.: Quantification of non-linearities as a function of time averaging in regional air quality modeling applications, *Atmos. Env.*, Vol. 103, ISSN 1352-2310, <https://doi.org/10.1016/j.atmosenv.2014.12.057>, 2015a.
- 765 Thunis, P., Pisoni, E., Degraeuwe, B., Kranenburg, R., Schaap, M., Clappier, A.: Dynamic evaluation of air quality models over European regions, *Atmos. Env.*, Vol. 111, ISSN 1352-2310, <https://doi.org/10.1016/j.atmosenv.2015.04.016>, 2015b.
- 770 Thunis, P., Clappier, A., Beekmann, M., Putaud, J. P., Cuvelier, C., Madrazo, J., and De Meij, A.: Non-linear response of PM<sub>2.5</sub> to changes in NO<sub>x</sub> and NH<sub>3</sub> emissions in the Po basin (Italy): consequences for air quality plans, *Atmos. Chem. Phys.*, 21, 9309–9327, <https://doi.org/10.5194/acp-21-9309-2021>, 2021a.



775 Thunis, P., Crippa, M., Cuvelier, C., Guizzardi, D., De Meij, A., Oreggioni, G., Pisoni, E.: Sensitivity of air quality modelling to different emission inventories: A case study over Europe, *Atmos. Env.*, X, Vol. 10, 100111, ISSN 2590-1621, <https://doi.org/10.1016/j.aeaoa.2021.100111>; <https://www.sciencedirect.com/science/article/pii/S2590162121000113>, 2021b.

780 Thunis, P., Clappier, A., Pisoni, E., Bessagnet, B., Kuenen, J., Guevara, M., and Lopez-Aparicio, S.: A multi-pollutant and multi-sectorial approach to screening the consistency of emission inventories, *Geosci. Model Dev.*, 15, 5271–5286, <https://doi.org/10.5194/gmd-15-5271-2022>, 2022.

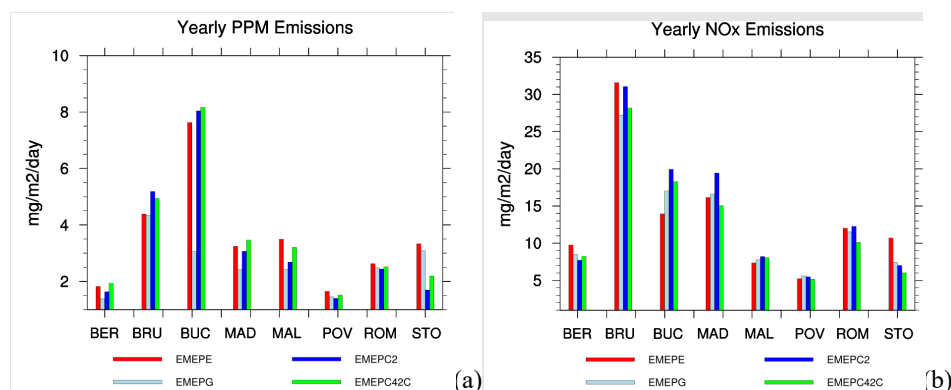
Trombetti, M., Thunis, P., Bessagnet, B., Clappier, A., Couvidat, F., Guevara, M., Kuenen, J., López-Aparicio, S.: Spatial inter-comparison of Top-down emission inventories in European urban areas, *Atmos. Env.*, Vol. 173, 785 ISSN 1352-2310, <https://doi.org/10.1016/j.atmosenv.2017.10.032>, 2018.

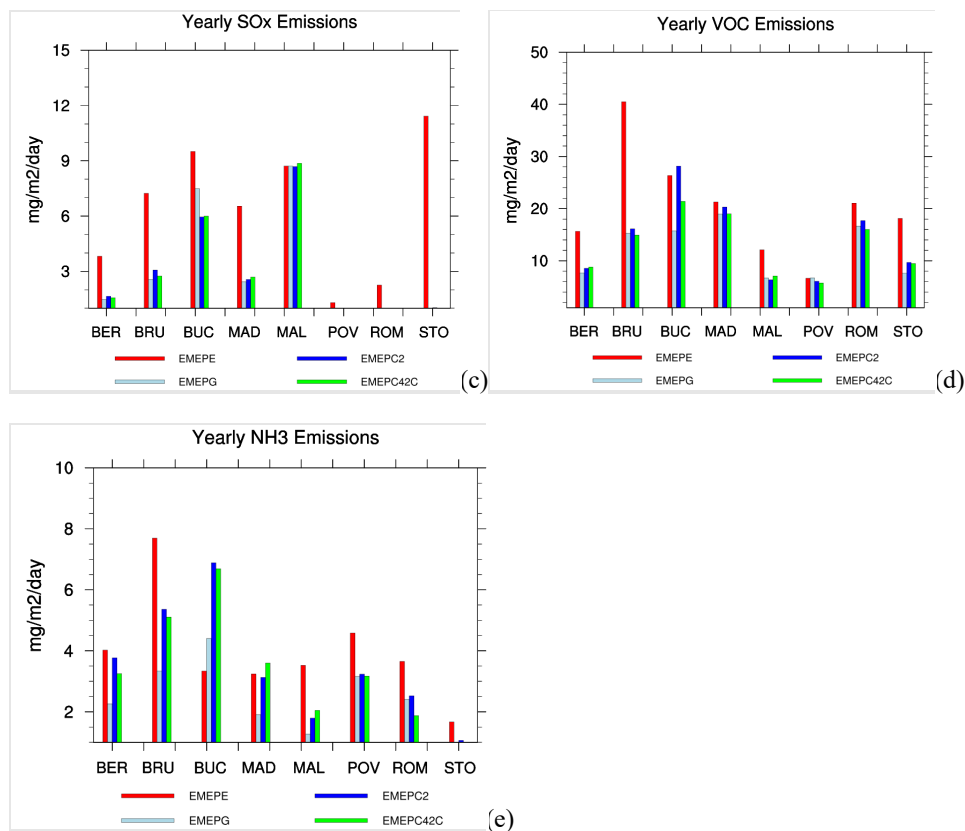
World Health Organization: WHO global air quality guidelines: particulate matter (PM<sub>2.5</sub> and PM<sub>10</sub>), ozone, nitrogen dioxide, sulfur dioxide and carbon monoxide. World Health Organization. <https://apps.who.int/iris/handle/10665/345329>. License: CC BY-NC-SA 3.0 IGO, 2021.

790 Xiao, X., Cohan, D. S., Byun, D. W., and Ngan, F.: Highly nonlinear ozone formation in the Houston region and implications for emission controls, *J. Geophys. Res.*, 115, D23309, doi:10.1029/2010JD014435, 2010.

795 Xing, J., Wang, S., Zhao, B., Wu, W., Ding, D., Jang, C., Zhu, Y., Chang, X., Wang, J., Zhang, F., Hao, J.: Quantifying Nonlinear Multi-regional Contributions to Ozone and Fine Particles Using an Updated Response Surface Modeling Technique. *Env. Sc. & Tech.*, 51, (20), 11788-11798, 2017.

800





805

Figure 1. Annual mean emission densities (mg/m<sup>2</sup>/day) for (a) PPM, (b) NOx, (c) SOx, (d) VOC and (e) NH<sub>3</sub> emissions by EMEPE (red), EMEPG (light blue), EMEPC2 (blue) and EMEPC42C (green), for the eight locations (Berlin [BER], Brussels [BRU], Bucharest [BUC], Madrid [MAD], Malopolska region [MAL], Po Valley region [POV], Rome [ROM] and Stockholm [STO]).

810

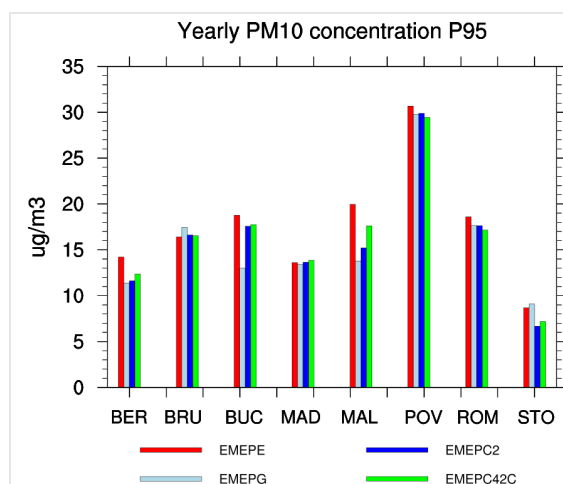


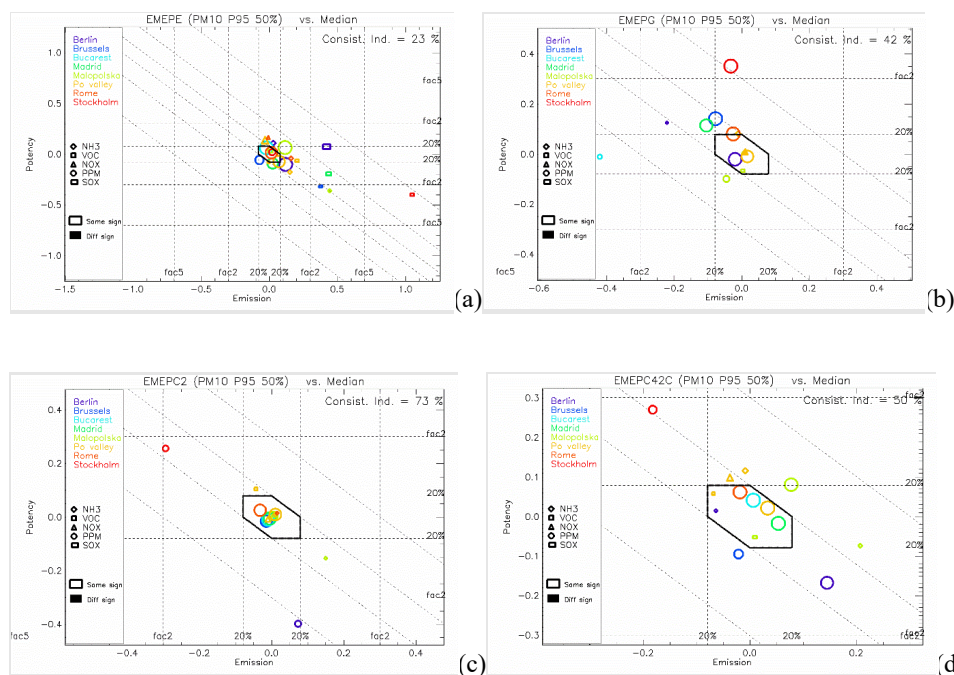
Figure 2. Total yearly average PM10 concentrations by EMEPE (red), EMEPG (light blue), EMEPC2 (blue) and EMEPC42C (green), for the eight locations (Berlin [BER], Brussels [BRU], Bucharest [BUC], Madrid [MAD],



815 Malopolska region [MAL], Po Valley region [POV], Rome [ROM] and Stockholm [STO]). The concentrations represent values above the 95 Percentile values, showing the highest 5% values in the domain from the BaseCase.

820

825



830 Figure 3. Diamond plot for PM10 concentrations for (a) EMEPE, (b) EMEPG, (c) EMEPC2 and (d) EMEPC42C. The values represent values above the 95 Percentile, showing the highest 5% values in the domain from the BaseCase. The X- and Y-axis are expressed as logarithms. For each city, the size of a symbol is proportional to the maximum absolute potential of the considered precursor, across models. Note that symbols for which emissions are relevant and that characterise the median all fall at the (0,0) position. For visualisation purpose, these have been slightly shifted within the diamond shape.

835

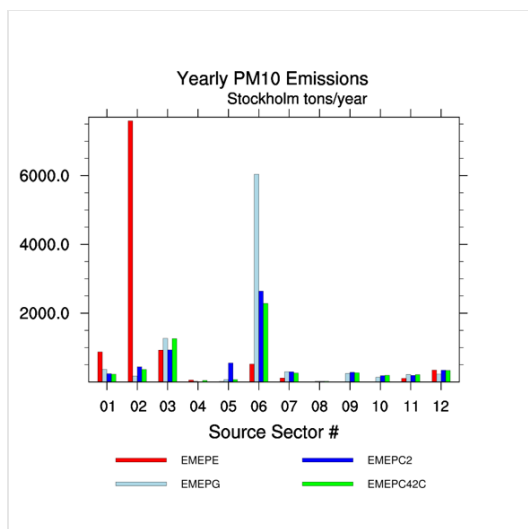
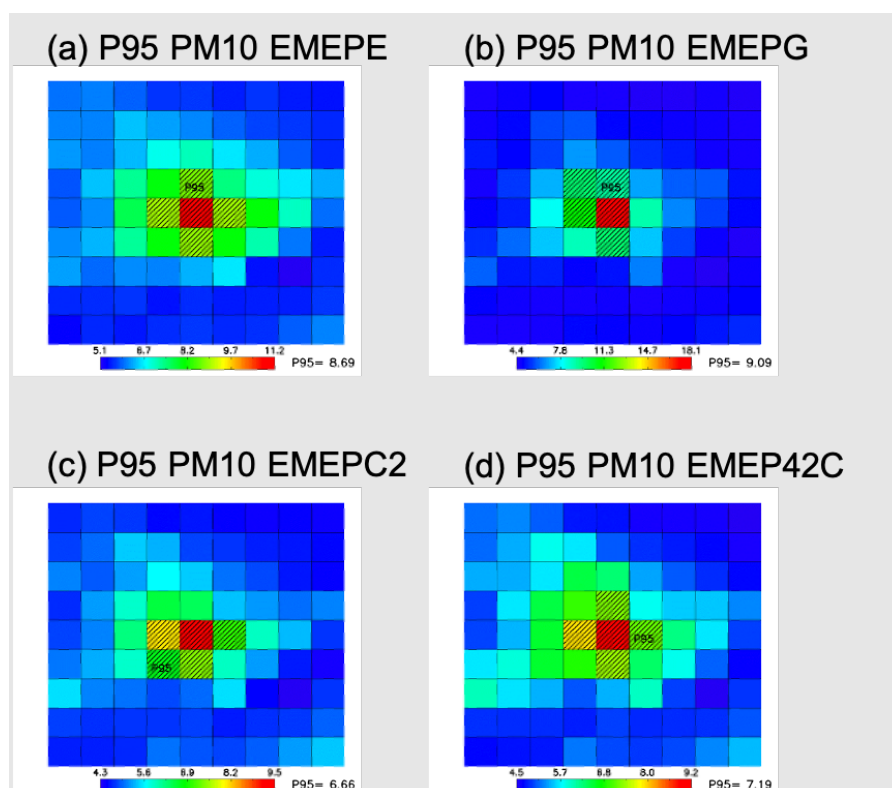


Figure 4. Total PM10 emissions (tons/year) for Stockholm for EMEPE (red), EMEPG (light blue), EMEPC2 (blue) and EMEPC42C (green).

840





845

Figure 5. Overview location P95 values for the calculated PM10 concentrations  $\mu\text{g}/\text{m}^3$  by the four Base Cases for domain STO. Shaded grid cells indicate the location of the values above the P95 by (a) EMEPE, (b) EMEPG, (c) EMEPC2 and (d) EMEPC42C. The number next to P95 represents the average of the P95 values.

850

Table 1(a) Overview of Base Case emissions ( $\text{mg}/\text{m}^2/\text{day}$ ) for NO<sub>x</sub> and SO<sub>x</sub>, together with the ratio in the emissions between these two pollutants. (b) Similar as to (a) but for potency at 95P in  $\mu\text{g}/\text{m}^3$ .

(a)

Emissions $\text{mg}/\text{m}^2/\text{day}$ NO <sub>x</sub>	Emissions $\text{mg}/\text{m}^2/\text{day}$				Ratio emissions SO <sub>x</sub> /NO <sub>x</sub>			
	EMEPE	EMEPG	EMEPC2	EMEPC42C	EMEPE	EMEPG	EMEPC2	EMEPC42C
Berlin	9.76	8.50	7.72	8.24	0.39	0.17	0.21	0.19
Brussels	31.57	27.21	31.05	28.16	0.23	0.09	0.10	0.10
Bucharest	13.94	17.01	19.93	18.28	0.68	0.44	0.30	0.33
Madrid	16.15	16.59	19.44	15.05	0.40	0.15	0.13	0.18
Malapolska	7.36	7.79	8.20	8.04	1.18	1.12	1.06	1.10
Po Valley	5.23	5.62	5.48	5.16	0.25	0.13	0.15	0.16
Rome	12.01	11.54	12.26	10.11	0.19	0.06	0.08	0.08
Stockholm	10.71	7.41	7.01	6.03	1.07	0.09	0.15	0.13

Emissions $\text{mg}/\text{m}^2/\text{day}$ SO <sub>x</sub>	Emissions $\text{mg}/\text{m}^2/\text{day}$			
	EMEPE	EMEPG	EMEPC2	EMEPC42C
Berlin	3.82	1.48	1.65	1.57
Brussels	7.23	2.56	3.07	2.75
Bucharest	9.51	7.49	5.95	6.00
Madrid	6.54	2.43	2.56	2.69
Malapolska	8.72	8.71	8.69	8.86
Po Valley	1.31	0.73	0.82	0.81
Rome	2.25	0.74	0.94	0.79
Stockholm	11.43	0.67	1.03	0.80

(b)

Potency P95 ( $\mu\text{g}/\text{m}^3/\text{ton}$ ) NO <sub>x</sub>	Potency P95 ( $\mu\text{g}/\text{m}^3/\text{ton}$ )				Ratio Potency SO <sub>x</sub> /NO <sub>x</sub>			
	EMEPE	EMEPG	EMEPC2	EMEPC42C	EMEPE	EMEPG	EMEPC2	EMEPC42C
Berlin	-0.0018	-0.0011	-0.0024	-0.0018	12.4	17.1	4.9	9.9
Brussels	0.0013	0.0013	0.0015	0.0012	-33.3	-36.2	-60.1	-42.7
Bucharest	-0.0067	-0.0047	-0.0019	-0.0017	7.1	12.8	36.2	43.5
Madrid	0.0002	-0.0002	-0.0002	-0.0013	-179.0	280.0	223.5	27.4
Malapolska	-0.001	-0.0011	-0.0004	-0.001	2.4	1.7	5.5	1.9
Po Valley	-0.0064	-0.0047	-0.0046	-0.0059	1.6	2.4	2.5	1.2
Rome	-0.022	-0.0076	-0.0151	-0.0089	2.7	15.9	4.6	13.5
Stockholm	-0.0011	-0.0011	-0.0006	-0.0005	18.8	30.5	86.3	81.2

Potency P95 ( $\mu\text{g}/\text{m}^3/\text{ton}$ ) SO <sub>x</sub>	Potency P95 ( $\mu\text{g}/\text{m}^3/\text{ton}$ )			
	EMEPE	EMEPG	EMEPC2	EMEPC42C
Berlin	-0.0223	-0.0188	-0.0117	-0.0178
Brussels	-0.0433	-0.0471	-0.0902	-0.0512
Bucharest	-0.0476	-0.06	-0.0687	-0.0739
Madrid	-0.0358	-0.056	-0.0447	-0.0356
Malapolska	-0.0024	-0.0019	-0.0022	-0.0019
Po Valley	-0.01	-0.0113	-0.0115	-0.0072
Rome	-0.0584	-0.1209	-0.0695	-0.1204
Stockholm	-0.0207	-0.0335	-0.0518	-0.0406

855

Table 2. Absolute potential (50%) divided by the Absolute potential (25%) for PM10 when NO<sub>x</sub> emissions are reduced by 50% and 25% for 95 Percentile values (P95). Numbers with a ratio higher than 3% compared to the PPM 50% Potential 95P are shown.

City	EMEPE	EMEPG	EMEPC2	EMEPC42C
BER011	1.17	1.19	1.09	1.14



BRU003	1.22		1.21	1.15
BUC006		1.18		
MAD004				
MAL001	1.17	1.14	1.29	1.20
POV002	1.21	1.27	1.42	1.24
ROM005	1.18	1.15	1.21	1.19
STO008				

860

**Table 3. Absolute potential (50%) divided by the Absolute potential (25%) for PM10 when VOC emissions are reduced by 50% and 25% for 95 Percentile values (P95). Numbers with a ratio higher than 3% compared to the PPM 50% Potential 95P are shown.**

City	EMEPE	EMEPG	EMEPC2	EMEPC42C
BER011				
BRU003				
BUC006				
MAD004	0.97		0.96	
MAL001				
POV002		0.97		0.99
ROM005				
STO008				

865

**Table 4. Absolute potential (50%) divided by the Absolute potential (25%) for PM10 when NH3 emissions are reduced by 50% and 25% for 95 Percentile values (P95). Numbers with a ratio higher than 3% compared to the PPM 50% Potential 95P are shown.**

City	EMEPE	EMEPG	EMEPC2	EMEPC42C
BER011	1.11	1.08	1.11	1.09
BRU003	1.09	1.11	1.09	1.11
BUC006	1.09	1.08	1.12	1.10
MAD004	1.15	1.09	1.12	1.13
MAL001	1.16	1.21	1.03	1.13
POV002	1.28	1.28	1.26	1.26
ROM005	1.15	1.13	1.16	1.14
STO008	1.13	1.15	1.10	1.04

870

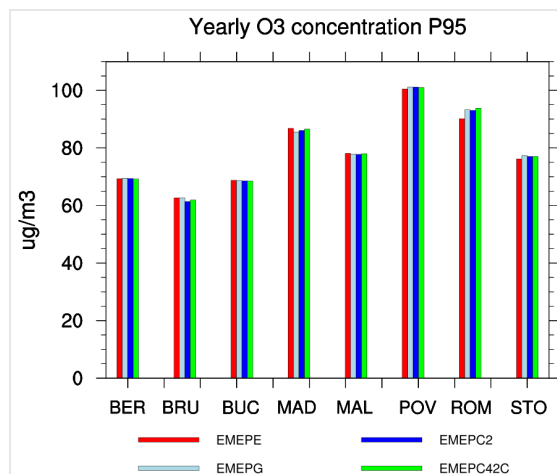
**Table 5. Absolute potential (50%) divided by the Absolute potential (25%) for PM10 when PM2.5 and PMcoarse emissions are reduced by 50% and 25% for 95 Percentile values (P95).**

City	EMEPE	EMEPG	EMEPC2	EMEPC42C
BER011	1.00	1.00	1.00	1.00
BRU003	1.00	1.00	1.00	1.00
BUC006	1.00	1.00	1.00	1.00
MAD004	1.00	1.00	1.00	1.00
MAL001	1.00	1.00	1.00	1.00
POV002	1.01	1.01	1.01	1.01
ROM005	1.00	1.00	1.00	1.00
STO008	1.00	1.00	1.00	1.00

**Table 6. Absolute potential (50%) divided by the Absolute potential (25%) for PM10 when ALL pollutants (SOx, NOx, VOC, NH3, PM2.5 and PMcoarse) emissions are reduced together by 50% and 25% for 95 Percentile values (P95). Numbers with more than 5% non-linearity are highlighted.**

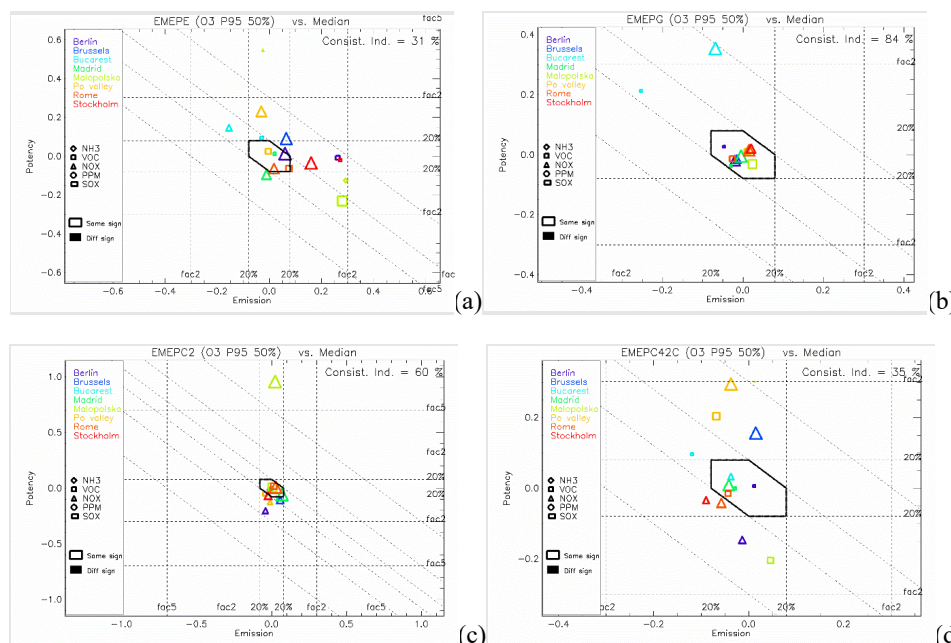
City	EMEPE	EMEPG	EMEPC2	EMEPC42C
BER011	1.01	1.24	1.02	1.01
BRU003	1.00	1.11	1.01	1.01
BUC006	1.01	1.19	1.01	1.00
MAD004	1.01	1.02	1.01	1.01
MAL001	1.01	1.07	1.01	1.01
POV002	1.02	1.05	1.02	1.00
ROM005	1.01	1.04	1.01	1.01
STO008	1.01	1.03	1.01	1.00

875



880

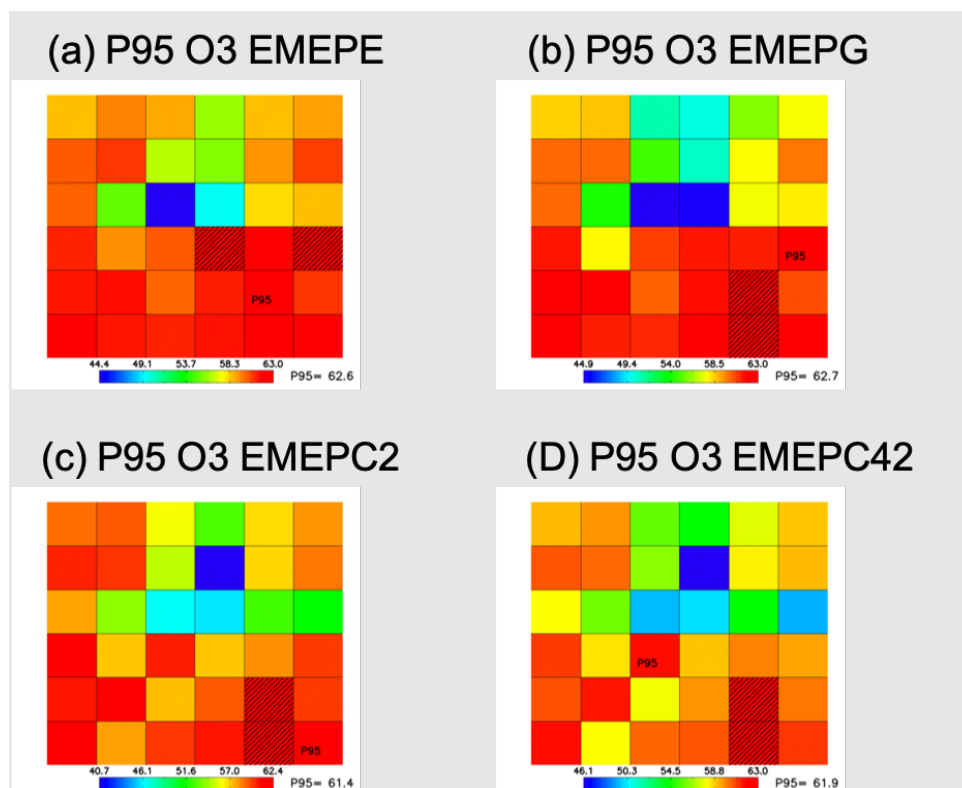
Figure 6. Yearly average O<sub>3</sub> concentrations by EMEPE (red), EMEPG (light blue), EMEPC2 (blue) and EMEPC42C (green), for the eight locations (Berlin, Brussels, Bucharest, Madrid, Malopolska region, Po Valley region, Rome and Stockholm). The concentrations represent values above the 95 Percentile values, showing the highest 5% values in the domain from the BaseCase.



885

Figure 7. Diamond plot for O<sub>3</sub> concentrations for (a) EMEPE, (b) EMEPG, (c) EMEPC2 and (d) EMEPC42C. The values represent values above the 95 Percentile, showing the highest 5% values in the domain from the BaseCase. The X- and Y-axis are expressed as logarithms. For each city, the size of a symbol is proportional to the maximum absolute potential of the considered precursor, across models. Note that symbols for which emissions are relevant and that characterise the median all fall at the (0,0) position. For visualisation purpose, these have been slightly shifted within the diamond shape.

890



895

Figure 8. Overview location P95 values for the calculated O3 concentrations  $\mu\text{g}/\text{m}^3$  by the four Base Cases for domain BRU. Shaded grid cells indicate the location of values above the P95 values by (a) EMEPE, (b) EMEPG, (c) EMEPC2 and (d) EMEPC42C. The number next to P95 represents the average of the P95 values.

900

Table 7(a) Overview of Base Case emissions ( $\text{mg}/\text{m}^2/\text{day}$ ) for NOx and VOC, together with the ratio in the emissions between these two pollutants. (b) Similar as to (a) but for potency at 95P in  $\text{mg}/\text{m}^3$ .

(a)

Emissions [ $\text{mg}/\text{m}^2/\text{day}$ ] NOx	Emissions [ $\text{mg}/\text{m}^2/\text{day}$ ]				Ratio Emissions VOC/NOx			
	EMEPE	EMEPG	EMEPC2	EMEPC42C	EMEPE	EMEPG	EMEPC2	EMEPC42C
BER011	9.76	8.50	7.72	8.24	1.60	0.90	1.11	1.07
BRU003	31.57	27.21	31.05	28.16	1.28	0.56	0.52	0.53
BUC006	13.94	17.01	19.93	18.28	1.89	0.92	1.41	1.17
MAD004	16.15	16.59	19.44	15.05	1.32	1.14	1.04	1.26
MAL001	7.36	7.79	8.20	8.04	1.65	0.86	0.78	0.88
POV002	5.23	5.62	5.48	5.16	1.27	1.20	1.11	1.11
ROM005	12.01	11.54	12.26	10.11	1.75	1.44	1.44	1.58
STO008	10.71	7.41	7.01	6.03	1.69	1.03	1.38	1.57

905

Emissions [ $\text{mg}/\text{m}^2/\text{day}$ ] VOC	Emissions [ $\text{mg}/\text{m}^2/\text{day}$ ]			
	EMEPE	EMEPG	EMEPC2	EMEPC42C
BER011	15.65	7.67	8.55	8.78



BRU003	40.50	15.29	16.13	14.93
BUC006	26.35	15.73	28.15	21.40
MAD004	21.28	18.97	20.31	19.00
MAL001	12.11	6.71	6.35	7.06
POV002	6.65	6.72	6.08	5.74
ROM005	21.05	16.66	17.69	16.02
STO008	18.13	7.63	9.69	9.46

(b)

Potency 95P ( $\mu\text{g}/\text{m}^3/\text{ton}$ )				
NOx 50%	EMEPE	EMEPG	EMEPC2	EMEPC42C
BER011	0.011	0.011	0.007	0.008
BRU003	0.063	0.051	0.040	0.073
BUC006	0.041	0.066	0.029	0.031
MAD004	0.013	0.016	0.014	0.017
MAL001	0.000	0.000	0.001	0.000
POV002	-0.003	-0.002	-0.001	-0.003
ROM005	0.044	0.051	0.052	0.046
STO008	0.013	0.014	0.012	0.013

Potency 95P ( $\mu\text{g}/\text{m}^3/\text{ton}$ )				
VOC 50%	EMEPE	EMEPG	EMEPC2	EMEPC42C
BER011	-0.003	-0.003	-0.003	-0.003
BRU003	-0.004	-0.006	-0.005	-0.006
BUC006	-0.013	-0.017	-0.010	-0.013
MAD004	-0.004	-0.003	-0.004	-0.003
MAL001	-0.001	-0.001	-0.001	-0.001
POV002	-0.001	-0.001	-0.001	-0.002
ROM005	-0.018	-0.021	-0.021	-0.021
STO008	-0.002	-0.003	-0.002	-0.002

910

**Table 8. Absolute potential (50%) divided by the Absolute potential (25%) for O<sub>3</sub> when NO<sub>x</sub> emissions are reduced by 50% and 25% for 95 Percentile values (P95). Numbers with more than 5% non-linearity are highlighted.**

City	EMEPE	EMEPG	EMEPC2	EMEPC42C
BER011	0.94	0.94	0.90	0.91
BRU003	1.00	1.00	1.00	1.01
BUC006	0.90	0.93	0.92	0.92
MAD004	0.87	0.88	0.88	0.88
MAL001	12.03	0.25	0.73	5.38
POV002	1.37	1.54	1.58	1.41
ROM005	0.91	0.93	0.93	0.92
STO008	0.93	0.92	0.91	0.91

915

**Table 9. Absolute potential (50%) divided by the Absolute potential(25%) for O<sub>3</sub> when VOC emissions are reduced by 50% and 25% for 95 Percentile values (P95).**

City	EMEPE	EMEPG	EMEPC2	EMEPC42C
BER011	1.00	1.00	1.01	1.01
BRU003	1.00	1.01	1.01	1.01
BUC006	1.01	1.01	1.01	1.01
MAD004	0.99	1.00	0.99	0.99
MAL001	1.02	1.01	1.01	1.02



POV002	1.04	1.02	1.03	1.03
ROM005	1.01	1.00	1.00	1.01
STO008	1.00	1.00	1.01	1.01

920 **Table 10. Absolute potential (50%) divided by the Absolute potential(25%) for O<sub>3</sub> when NO<sub>x</sub> and VOC emissions are reduced together by 50% and 25% for 95 Percentile values (P95). Numbers with more than 5% non-linearity are highlighted.**

City	EMEPE	EMEPG	EMEPC2	EMEPC42C
BER011	0.96	-1.40	0.90	0.92
BRU003	1.00	2.35	1.00	1.01
BUC006	0.92	0.76	0.94	0.94
MAD004	0.87	0.69	0.88	0.89
MAL001	1.63	0.40	0.74	1.46
POV002	1.17	1.57	1.19	1.17
ROM005	0.91	0.86	0.94	0.92
STO008	0.94	0.77	0.91	0.91